Geophysical Research Letters

RESEARCH LETTER
10.1029/2018GL077252

Key Points:
- A decade of continuous GPS data is used to study the connection between runoff and ice flow on a High Arctic glacier
- Enhanced ablation speeds up summer flow and slows down fall and winter motion; spring flow is largely insensitive to summer ablation
- Despite changes in the seasonal velocity pattern, the impact of increased runoff on annual mean velocities is insignificant

Supporting Information:
- Supporting Information S1

Correspondence to:
W. J. J. van Pelt,
ward.van.pelt@geo.uu.se

Citation:
van Pelt, W. J. J., Pohjola, V. A., Pettersson, R., Ehwald, L. E., Reijmer, C. H., Boot, W., & Jakobs, C. L. (2018). Dynamic response of a High Arctic glacier to melt and runoff variations. *Geophysical Research Letters*, *45*, 4917–4926. https://doi.org/10.1029/2018GL077252

Received 25 JAN 2018
Accepted 4 MAY 2018
Accepted article online 11 MAY 2018
Published online 28 MAY 2018

Dynamic Response of a High Arctic Glacier to Melt and Runoff Variations

Ward J. J. van Pelt[1], Veijo A. Pohjola[1], Rickard Pettersson[1], Lena E. Ehwald[1], Carleen H. Reijmer[2], Wim Boot[2], and Constantijn L. Jakobs[2]

[1]Department of Earth Sciences, Uppsala University, Uppsala, Sweden, [2]Institute for Marine and Atmospheric Research Utrecht, Utrecht University, Utrecht, Netherlands

Abstract The dynamic response of High Arctic glaciers to increased runoff in a warming climate remains poorly understood. We analyze a 10-year record of continuous velocity data collected at multiple sites on Nordenskiöldbreen, Svalbard, and study the connection between ice flow and runoff within and between seasons. During the melt season, the sensitivity of ice motion to runoff at sites in the ablation and lower accumulation zone drops by a factor of 3 when cumulative runoff exceeds a local threshold, which is likely associated with a transition from inefficient (distributed) to efficient (channelized) drainage. Average summer (June–August) velocities are found to increase with summer ablation, while subsequent fall (September–November) velocities decrease. Spring (March–May) velocities are largely insensitive to summer ablation, which suggests a short-lived impact of summer melt on ice flow during the cold season. The net impact of summer ablation on annual velocities is found to be insignificant.

Plain Language Summary A major uncertainty in future predictions of glacier mass loss, and the corresponding sea level rise contribution, stems from a lack of understanding of potential feedbacks between surface melt and ice motion. Melt water penetrating to the bed of a glacier facilitates fast ice motion through sliding. Whether increased melt water input induces a net long-term acceleration or deceleration of ice flow however critically depends on the interaction between melt input and transience of the subglacial drainage system at both intraseasonal and interseasonal time scales. To assess this, long-term data sets of ice motion and runoff are essential. In this study, a 10-year record of continuous velocity data, collected at multiple sites on Nordenskiöldbreen in Svalbard, is presented and compared to simulated runoff. We find that the sensitivity of summer velocities to runoff drops by a factor of 3 after a runoff-induced change of drainage system morphology. While average summer motion increases with ablation, fall (September–November) motion decreases, and spring (March–May) motion appears largely insensitive to summer melt. Altogether, the net impact of increased summer melt on annual velocities is found to be negligible.

1. Introduction

A major uncertainty in future predictions of mass change of glaciers and ice sheets, and thereby the cryospheric contribution to sea level rise, stems from a lack of constraints on transient ice dynamics in a warming climate (Church et al., 2013). The connection between surface runoff, subglacial hydrology, and basal lubrication has been widely acknowledged (Clarke, 2005). Initial suggestions of a positive long-term relation between ice flow velocities and runoff (Parizek & Alley, 2004; Zwally et al., 2002) would imply the potential for accelerated mass loss as ice is transported more efficiently to lower elevations. However, this disregards changes of the drainage system in response to variable runoff, which in recent years has been shown to be the decisive component in explaining both short-term (intraseasonal) and long-term (interannual to decadal) velocity variations of land-terminating glaciers (e.g., Bartholomew et al., 2012; Sole et al., 2013; Tedstone et al., 2015; Van de Wal et al., 2015).

Runoff in the early melt season drains to the bed via moulins and crevasses, thereby pressurizing the distributed (linked-cavity) drainage system. A reduced effective pressure speeds up basal sliding, resulting in a characteristic early melt season velocity peak (e.g., Lliboutry, 1968). As surface melting and runoff intensifies

during the melt season, the drainage system expands, and when discharge exceeds a critical threshold (Kamb, 1987; Walder, 1986), the drainage system transforms into a more efficient channelized drainage system (e.g., Bingham et al., 2005; Hock & Hooke, 1993; Nienow et al., 1998; Röthlisberger, 1972), operating at low water pressure and draining water from the connected distributed drainage system (Andrews et al., 2014; Cowton et al., 2016; Hubbard et al., 1995).

Based on steady state theory of conduit flow (Kamb, 1987; Röthlisberger, 1972), it has been concluded that long-term slowdown of summer velocities could potentially result from extended periods of channelized drainage and low water pressure in a warmer climate (Bingham et al., 2003; Sundal et al., 2011; Van de Wal et al., 2008). Conversely, it has been argued that steady state theory is unlikely to apply, because rapid fluctuations in runoff entering a slowly adapting drainage system can lead to sudden water pressure fluctuations, thereby explaining melt-induced velocity peaks even during channelized drainage (e.g., Bartholomaus et al., 2008; Bartholomew et al., 2012; Kamb et al., 1994). High summer melt rates have been shown to coincide with below-average winter motion (Burgess et al., 2013; Sole et al., 2013), which has recently been linked to the action of weakly connected distributed drainage regions that gradually drain during the melt season and only slowly refill and repressurize after the melt season (Andrews et al., 2014; Hoffman et al., 2016).

The long-term impact of increased runoff on ice velocity of land-terminating glaciers remains unclear. A multidecadal decline in ice flow has been observed in conjunction with increased melt in Greenland (Tedstone et al., 2015; Van de Wal et al., 2015), but it remains uncertain the extent to which this slowdown is hydrologically induced or related to other factors, such as changes in ice geometry (Stevens et al., 2016), which also explained slowdown of glaciers in Alaska (Waechter et al., 2015) and the Canadian Arctic (Thomson & Copland, 2017). Correlations between annual velocities and summer melt are generally insignificant (Stevens et al., 2016; Van de Wal et al., 2015) but may be the result of opposing sensitivities of summer and winter velocities to melt (Sole et al., 2013).

The focus area of this study is the Svalbard archipelago, where feedbacks related to sea ice retreat cause the climate to change at an amplified rate compared to the global mean (Bintanja et al., 2011; Serreze et al., 2009). Recent warming has induced glacier thinning (James et al., 2012) and retreat, resulting in a 7% reduction of glacier area between 1983 and 2013 for a set of ~400 glaciers (Nuth et al., 2013). Previous work linking glacier flow in Svalbard to runoff has mostly focused on understanding the dynamic behavior of surge-type glaciers (e.g., Dunse et al., 2015; Nuttall & Hodgkins, 2005; Oerlemans & Van Pelt, 2015; Sevestre & Benn, 2015), which behave largely independently of the climate forcing (Evans & Rea, 1999). To date, knowledge about the dynamic response of polythermal, nonsurging glaciers in the High Arctic to transient runoff remains limited (Bingham et al., 2005; Irvine-Fynn et al., 2011; Vallot et al., 2017), both at short (intraseasonal) and long (interseasonal) time scales. This generates considerable uncertainty in the dynamic component of mass loss of these glaciers in a rapidly warming Arctic environment.

This paper presents a data set of continuous Global Positioning System (GPS) velocities, collected at 11 sites on Nordenskiöldbreen, a nonsurging, polythermal and (primarily) land-terminating glacier in central Svalbard. Collection and processing of the GPS data on Nordenskiöldbreen has previously been discussed in Den Ouden et al. (2010), together with a discussion of velocity time series between 2006 and 2009. Here we analyze 10 years (2006–2016) of velocity data and compare with simulated runoff and observed stake ablation. The length of the continuous measurement record allows for a detailed assessment of the connection between ice flow and inferred surface runoff at both intraseasonal and interseasonal time scales.

2. Study Area

Nordenskiöldbreen is a ~25-km-long outlet glacier of the Lomonosovfonna ice cap in central Spitsbergen (Figure 1). The main flow between De Geerfjellet and Terrierfjellet merges with two main tributaries to the south. Medial moraines originating at the western tips of Terrierfjellet and Ferrierfjellet indicate the long-term ice flow trajectory (Figure 1). The front of Nordenskiöldbreen has retreated by 15–35 m/a since the end of the Little Ice Age, but retreat rates have been negligible since ~2002 as the glacier is retreating on land (Allaart, 2016; Rachlewicz et al., 2007). The glacier covers an elevation range from sea level to about 1200 m above sea level (asl), and largest ice thickness (up to around 600 m) is found in an overdeepening between Terrierfjellet and De Geerfjellet (Figure 1; Van Pelt et al., 2013). The surface mass balance between 1989 and 2010 was −0.39 m w.e. (water equivalent) per year and the equilibrium line altitude (ELA) was estimated at 719 m asl

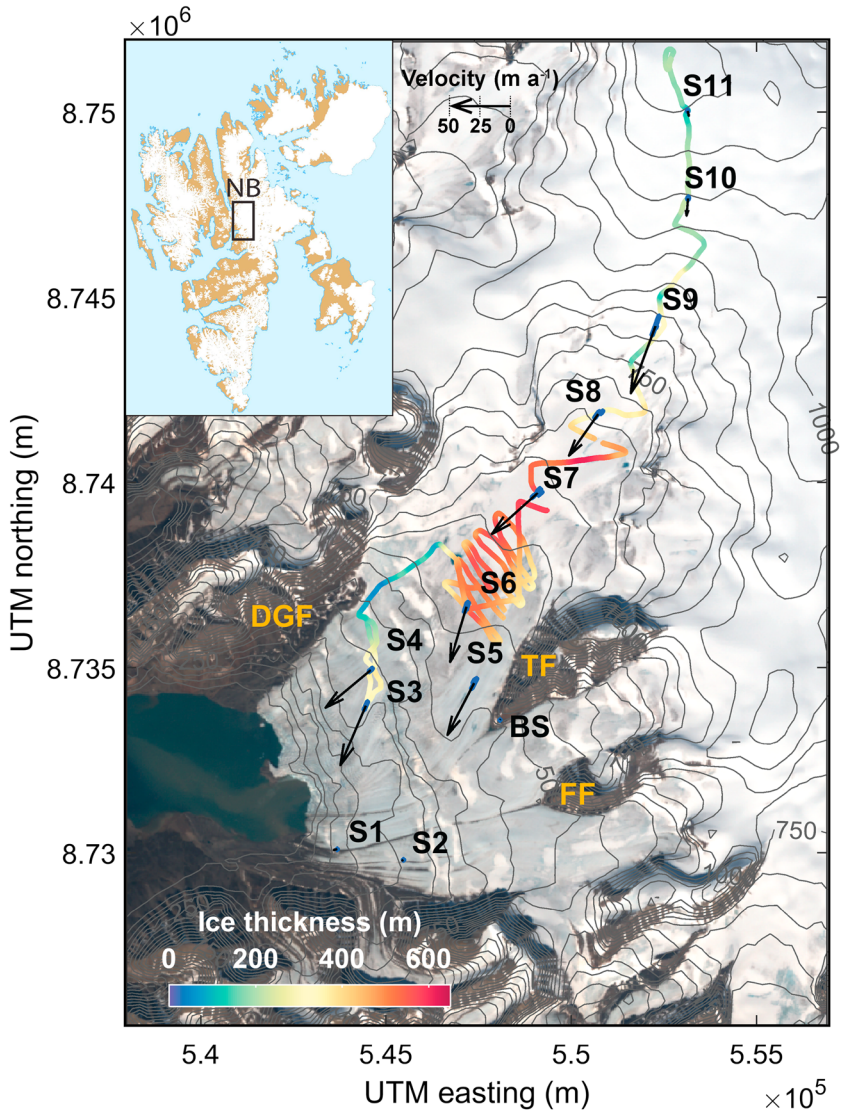

Figure 1. Satellite and elevation contour map of Nordenskiöldbreen. The inset panel shows Svalbard with the approximate location of Nordenskiöldbreen (black box). Elevation contours relative to sea level are drawn every 50 m (Norwegian Polar Institute Map Data and Services). Continuous GPS positions (blue) were measured at sites S1–S11. A reference station (BS) is installed on Terrierfjellet. Black arrows indicate mean ice flow, with arrow length proportional to absolute velocity (maximum 59 m/a at S9). Ice thickness along ground-penetrating radar tracks in 2010 is shown in the background (Van Pelt et al., 2013). The satellite map is from National Aeronautics and Space Administration Landsat 7 imagery taken on 13 July 2002. UTM coordinates are in UTM zone 33×. DGF = De Geerfjellet; TF = Terrierfjellet; FF = Ferrierfjellet.

(Van Pelt et al., 2012). Nordenskiöldbreen is a polythermal glacier ("type b" in Blatter & Hutter, 1991), with temperate conditions in the accumulation zone due to deep meltwater percolation and refreezing (Marchenko et al., 2016, 2017; Vega et al., 2016), and cold near-surface ice in the ablation area (Van Pelt et al., 2012). Unlike neighboring outlet glacier Tunabreen, Nordenskiöldbreen is not a surge-type glacier, at least no surges have occurred since the termination of the Little Ice Age according to analysis of foreland landforms (Ewertowski et al., 2016).

3. Data and Methods

Stand-alone GPS units have been mounted on stakes, drilled into the snow or ice, at 11 sites on Nordenskiöldbreen, measuring hourly positions since 2006 (Figure 1; Den Ouden et al., 2010). Long-term mean velocities were calculated for all stakes (S1–S11), while time series of 10-day velocities were determined

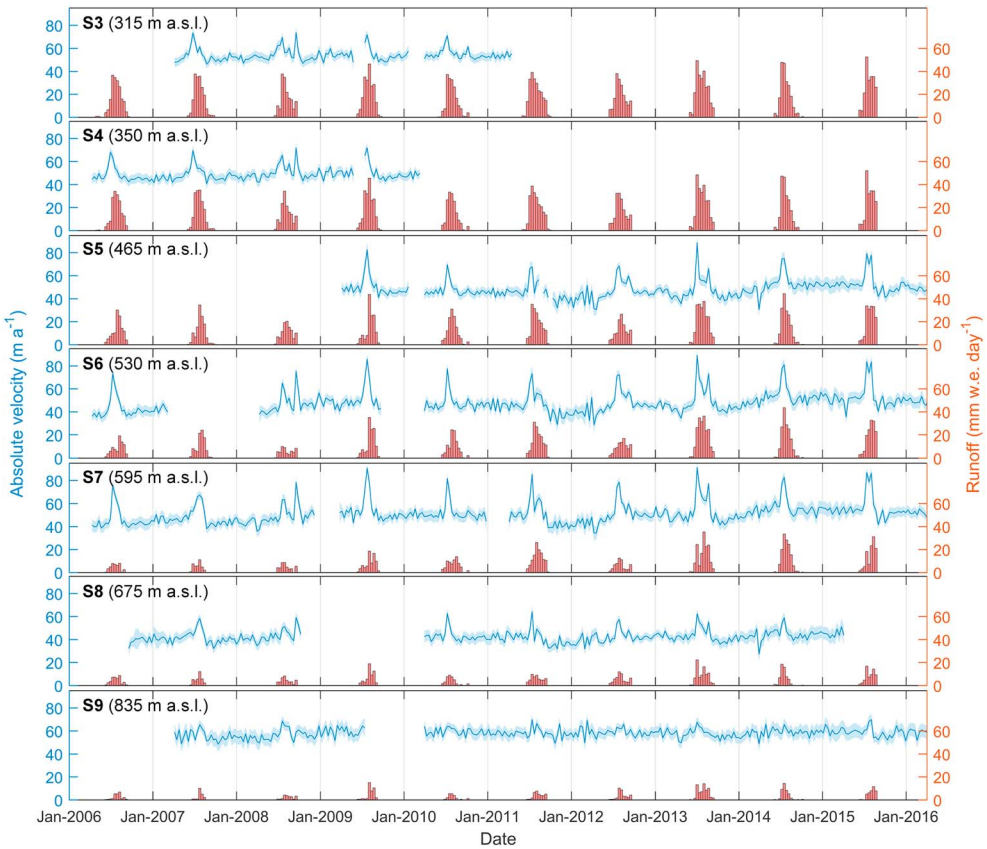

Figure 2. Time series of 10-day absolute velocity (left axis) and simulated runoff (right axis) between 2006 and 2016 for sites S3 to S9 (top to bottom). Light blue error bars indicate 95% confidence intervals for the 10-day velocities. asl = above sea level.

only for fast-moving stakes (40 m/a) S3 to S9, for which intraseasonal and interseasonal velocity variability well exceeded estimated errors of 10-day velocities of 1.5–4.9 m/a (Figure 2). More details on the processing steps and data quality are discussed in the supporting information (Text S1 and Figures S1 and S2; Andersen et al., 2010; Nettles et al., 2008).

Point summer balance and ELA are calculated from annual stake readings along with snow depth measurements around the stake (Van Pelt et al., 2012; Van Pelt, Kohler, et al., 2016). Stake summer balance is calculated using information of spring surface height and end-of-summer surface height, estimated by subtracting snow depth from surface height in the subsequent spring measurement. In the accumulation zone, refreezing above the summer surface is implicitly accounted for by assuming an end-of-summer remaining snow density of 550 kg/m^3. ELA is estimated per year by polynomial interpolation to find the zero-mass-balance elevation. ELA uncertainty is estimated at 55 m, based on a balance gradient of 0.003 m w.e.$\cdot$a$^{-1}\cdot$m^{-1} and a point mass balance uncertainty of 0.17 m w.e./a (Van Pelt et al., 2012, 2014).

Runoff at GPS sites is simulated with the coupled energy balance firn model EBFM (Van Pelt et al., 2012). Driven by meteorological fields from the regional atmospheric climate model RACMO2 (Noël et al., 2015), the surface energy balance model solves for glacier surface temperature and estimates surface melt. The firn model accounts for vertical transport, storage, and refreezing of melt and rain water, while tracking the evolution of subsurface density, temperature, and water content. Here runoff refers to downward water flow at the base of the snow/firn column, if present, or at the surface. Runoff is simulated with a 3-hourly resolution; 10-day sums are determined for comparison with velocity time series. More details about EBFM, the meteorological forcing, model calibration, and validation are given in the supporting information (Text S2 and Figure S3; Dee et al., 2011; Van Pelt & Kohler, 2015; Vega et al., 2016; Van Pelt, Pohjola, & Reijmer, 2016).

4. Results and Discussion

The following section presents and discusses the connection between ice flow and runoff/ablation at both intraseasonal (section 4.1) and seasonal (section 4.2) time scales.

4.1. Intraseasonal Velocities

GPS units at S1 and S2 were deployed on a southerly tributary flow and exhibit slow movement (∼1–3 m/a) due to low mass turnover and high lateral drag (Figure 1). All other GPS units (S3 to S11) are located along or close to the main flow line of Nordenskiöldbreen. High velocities are recorded in the ablation zone and lower accumulation zone at S3 to S9 with average speeds for the whole period ranging from 42 (S8) to 59 m/a (S9). Fastest mean ice flow is observed at S9 and explained by a combination of flow convergence and high surface slope, induced by steep gradients in the bed topography (Figure 1; Van Pelt et al., 2013). Higher up in the accumulation zone, velocities decrease with average speeds of 14 m/a at S10 and 4 m/a at S11.

Time series of 10-day velocities at S3 to S9 typically reveal an early melt season peak, above-average velocities throughout summer, and relatively stable lower velocities during the remainder of the year (Figure 2). A decrease in magnitude of summer speed up with elevation is apparent between S7 to S9 and coincides with a strong decline in runoff around the ELA at ∼700 m asl. A weak delay between melt season velocity peaks with increasing elevation is apparent (∼10–20 days between S3 and S9), but exact quantification is hampered by the coarse 10-day temporal resolution of the data. Velocity maxima typically occur in June or early July and in all years, except 2008, are found to precede or coincide with runoff maxima.

In order to investigate the relation between intraseasonal velocities and runoff, local velocity anomalies (relative to the mean for a stake over the entire observation period) at S3 to S9 are compared against 10-day runoff (Figure 3). The local cumulative runoff for each velocity anomaly is indicated by the marker color. Figure 3 suggests a transition from a period with high sensitivity of velocity to runoff in the early melt season to a period with much lower sensitivity to runoff later in the melt season. To determine the cumulative runoff at which this transition occurs, two linear regressions were performed: one for data above and one for data below a cumulative threshold value. A range of possible threshold values were tested to find the value (440 mm w.e.) with the highest mean correlation for the two regressions. Based on previous work, we argue that the decline of sensitivity of velocity to runoff around this threshold is likely to arise from a change in drainage morphology from a low-efficiency distributed drainage system to a highly efficient channelized system (e.g., Bartholomaus et al., 2008; Cowton et al., 2016; Iken, 1981; Kamb et al., 1994). Slopes of the linear regressions (β) represent the sensitivity of flow velocity to runoff during the early melt season, that is, prior to channelization, and during the late melt season, that is, after channelization (Figure 3). For S3–S9, we find an early melt season sensitivity of 1.34 ± 0.15 m/a per mm·w.e.·day^{-1} ($R = 0.70$; $P < 0.001$), compared to a late melt season sensitivity of 0.44 ± 0.07 m/a per mm·w.e.·day^{-1} ($R = 0.61$; $P < 0.001$). Hence, we conclude that the sensitivity of velocity to runoff during highly efficient channelized drainage is only $33 \pm 10\%$ of the sensitivity during less-efficient distributed drainage.

Below the cumulative runoff threshold, we infer that any runoff is primarily stored in englacial voids (moulins and crevasses), thereby raising the water pressure and allowing for gradual expansion of subglacial cavities in response to reduced creep closure and increased sliding-induced cavitational opening (Bueler & van Pelt, 2015; Werder et al., 2013). During early-season distributed drainage, we expect water transport rates in the subglacial system are small, which implies that new surface input primarily raises the englacial water level and water pressure, while short periods of low input have a smaller (negative) impact on water pressure. As water pressure reaches and remains close to overburden pressure for some time, coincident with the occurrence of the early melt season velocity peak, it can be argued that cavity expansion causes a gradual increase in horizontal discharge until it reaches a critical value at which unstable cavity growth through wall melt enforces channelization (Flowers, 2008; Kamb, 1987; Schoof, 2010; Walder, 1986). Since it is mostly local runoff that determines the water pressure prior to channelization, we argue that a cumulative runoff threshold, in addition to critical discharge, can be regarded as a predictor for the timing of channelization.

The cumulative runoff threshold is likely to vary spatially, due, for example, to variability in ice thickness affecting the rate of creep closure. Hence, the cumulative runoff threshold of 440 mm w.e. should be regarded as a spatial average. Spatial dependence of the cumulative runoff threshold becomes apparent when repeating the calculation of the threshold for two subsets of the data (S3–S6 and S7–S9) resulting in cumulative runoff thresholds of 410 (S3–S6) and 600 (S7–S9) mm w.e. As runoff rates decrease with elevation,

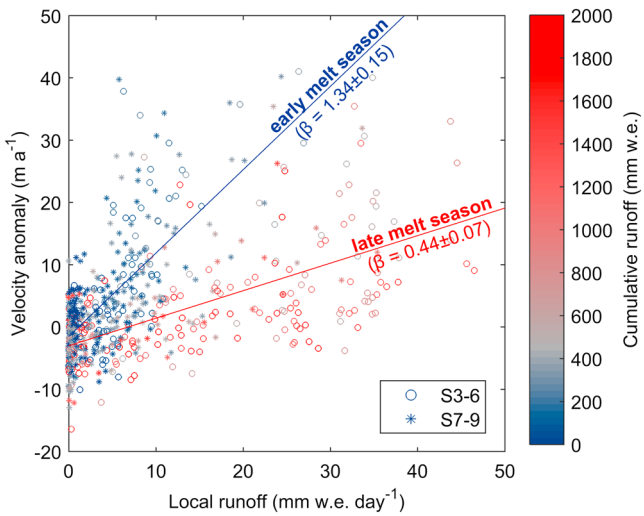

Figure 3. Comparison of 10-day velocity anomalies and local runoff for S3 to S9 between 2006 and 2016. Cumulative runoff for each velocity anomaly is indicated by the marker color. Linear regressions for the early melt season (cumulative runoff <440 mm w.e.; solid blue line) and late melt season (cumulative runoff >440 mm w.e.; solid red line) are shown; trend slopes (β) and 95% confidence limits are given. w.e. = water equivalent.

with a most pronounced decline around the ELA, channelization is delayed at higher elevations or may not occur when cumulative runoff does not exceed the threshold. During the 10-year observation period, the cumulative runoff threshold (440 mm w.e.) was exceeded in all years at S3 to S6 (315–530 m asl), during 7 years at S7 (595 m asl), 6 years at S8 (675 m asl), and only 1 year (2013) at S9 (835 m asl).

We find a weak but positive correlation between velocity and runoff during channelized drainage (cumulative runoff >440 mm w.e.), which has previously also been found by Bartholomew et al. (2010) and was ascribed to short-term (daily) peaks in runoff, causing short-lived pressurization of the channelized and adjacent distributed system. Fast ice flow during channelized drainage may occur in response to high short-term runoff variability, since cavity expansion in the connected distributed system adds a forward component to ice flow, while cavity closure is more downward (Cowton et al., 2016; Iken, 1981). It has been argued that steady state theory, suggesting an inverse relation between runoff and water pressure during channelized drainage, is unlikely to apply in environments with rapid variations in runoff (Bartholomew et al., 2012; Cowton et al., 2016; Hewitt, 2013; Kehrl et al., 2015). Since we find a strong positive correlation of 10-day runoff and the variance of daily runoff within 10-day intervals ($R = 0.79$; $P < 0.001$), we expect that the positive relation between runoff and velocity at a 10-day time scale may well be the result of runoff fluctuations at time scales shorter than 10 days.

4.2. Seasonal Velocities

Next, we shift our focus to the longer seasonal time scales and discuss the impact of summer mass balance on summer and winter velocity. Point mass balance observations provide data of summer mass balance at GPS sites and are also used to extract time series of ELA (section 3). Seasonal mean velocities per stake are calculated for summer (June–August, JJA), fall (September–November, SON), winter (December–February), and spring (March–May). To facilitate calculating correlations between seasonal velocities and summer balance for all stakes (Figures 4a and 4b), normalized seasonal velocities are determined (by dividing by the long-term seasonal mean at individual sites), and compared with summer balance anomalies (determined by subtracting the long-term mean summer balance at individual sites). This is done for GPS sites S5 to S9, for which at least 5 years of data were available. Note that a positive (negative) summer balance anomaly at a site implies a negative (positive) ablation anomaly, that is, less (more) melt, relative to the long-term mean.

Comparing normalized summer velocity (JJA) and summer balance anomaly at S5–S9 (Figure 4a) reveals a significant negative trend of −8% per m w.e. a^{-1} ($R = -0.44$; $P < 0.01$) for all data. This suggests above-average summer velocity during high-melt summers. Based on the found positive intraseasonal relations between runoff and velocity (section 4.1) both a longer duration of the runoff season and higher intensity of runoff events are likely to enhance ice flow during warm summers.

A comparison of normalized fall (SON) velocities and summer balance anomaly at individual sites (Figure 4b) reveals a significant positive trend of 10% per m w.e. a^{-1} ($R = 0.49$; $P < 0.01$) for all data points. This suggests that high-melt summers generally induce below-average fall motion, in line with previous findings in Greenland (e.g., Sole et al., 2013; Van de Wal et al., 2015). One possible explanation for this is given by Andrews et al. (2014) and Hoffman et al. (2016), who ascribe reduced late melt season and winter velocities to gradual drainage of weakly connected parts of the distributed drainage system during the melt season and slow refilling and repressurization of these regions during the subsequent cold season. Alternatively, Sole et al. (2013) and Tedstone et al. (2015) ascribed reduced winter velocities after high-melt summers to more widespread channelized drainage, inducing low water pressures across a larger fraction of the bed. Interestingly, we find that the correlation between summer balance anomaly and seasonal ice motion drops over the course of the cold season to $R = 0.43$ ($P = 0.01$) in winter (December–February) and to an insignificant value of $R = 0.14$ ($P > 0.05$) in spring (March–May). This drop in correlation suggests that the influence of summer ablation on subglacial conditions after the melt season is typically a few months.

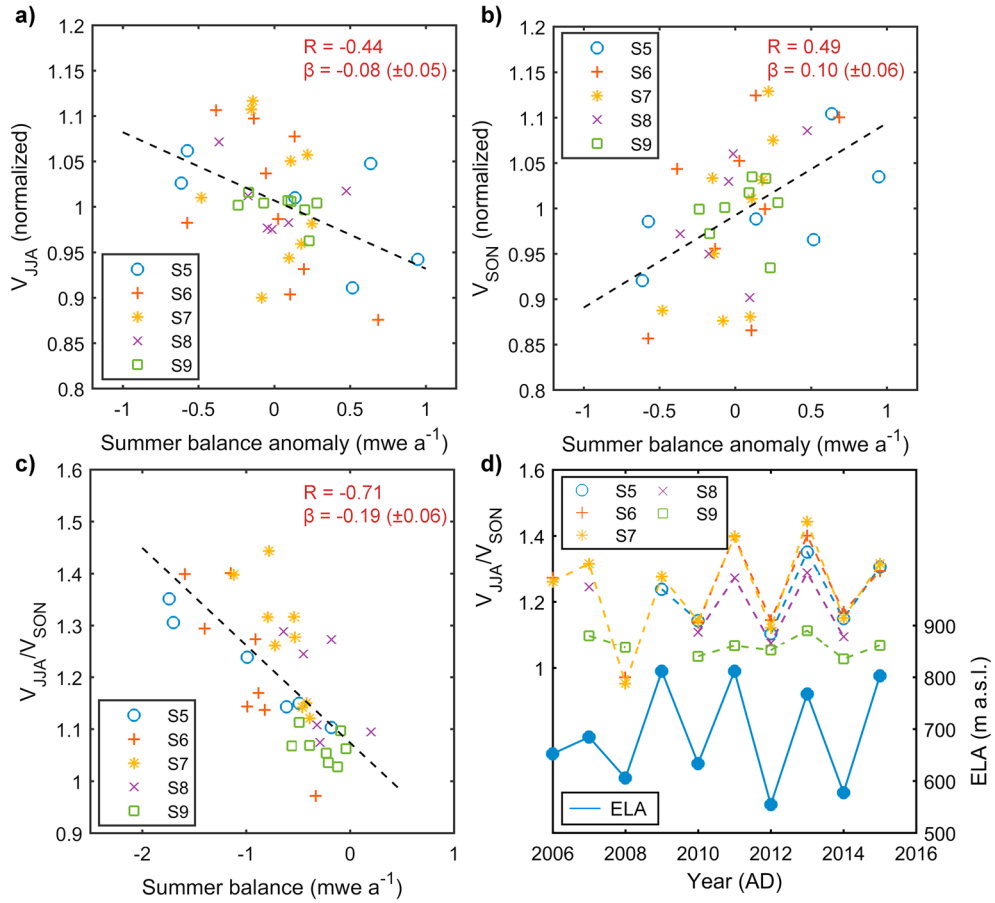

Figure 4. Normalized summer (a) and fall (b) velocity as a function of summer balance anomaly at S5 to S9. Panel (c) shows V_{JJA}/V_{SON} as a function of summer balance. Time series of V_{JJA}/V_{SON} for individual stakes (left axis) and ELA (right axis) are shown in (d). Trend slopes (β) in (a)–(c) are in (m w.e.)$^{-1}$ a with 95% confidence limits given in brackets. JJA = June–August; SON = September–November; ELA = equilibrium line altitude; asl = above sea level.

We find no evidence for runoff-induced flow acceleration or deceleration in a warming climate, since opposing trends during and after the summer season cause normalized annual velocities, determined for years starting 1 June, to be insignificantly correlated to summer balance anomaly ($R = 0.10$; $P > 0.05$). Nevertheless, a strong anticorrelation is found between the ratio of summer and fall velocity (V_{JJA}/V_{SON}) and summer balance ($R = -0.71$; $P < 0.001$; Figure 4c), which suggests amplification of the seasonal velocity cycle in a warming climate. A mean trend of −0.19 per m w.e. a^{-1} is found, which is equivalent to a 19% increase of V_{JJA}/V_{SON} for a 1-m w.e./a increase in summer ablation. Finally, time series of V_{JJA}/V_{SON} at S5–S9 and ELA are compared in Figure 4d, revealing very similar temporal patterns. A pronounced decrease in magnitude and temporal variability of V_{JJA}/V_{SON} is apparent between sites in the ablation zone (S5–S8) and the lower accumulation zone (S9), which is explained by a sharp contrast of runoff and its interannual variability around the ELA. Upward migration of the ELA in a warming climate may therefore be expected to enhance and extend the seasonal velocity cycle to higher elevations.

5. Conclusions

Using a decade of GPS velocity data, modeled runoff and observed summer balance, we analyzed the connection between ice flow and surface runoff/ablation on Nordenskiöldbreen, Svalbard, at both intraseasonal and seasonal time scales. During the melt season a transition from inefficient (distributed) drainage to efficient (channelized) drainage is found to occur when cumulative runoff exceeds a local threshold. We find a positive dependence of velocity to runoff throughout the melt season, however, velocities are found to be 3 times more sensitive to runoff variability during distributed drainage than during channelized drainage. Our results

confirm that steady state theory, suggesting an inverse relationship between runoff and water pressure for channelized drainage is unlikely to apply in environments with rapid variations in runoff.

Comparing interannual variability of seasonal velocity and stake summer balance reveals a significant positive correlation between summer ablation and summer velocity, while a negative correlation is found between fall velocity and summer ablation. Spring velocities are found to be insensitive to summer ablation, thereby suggesting a relatively short-lived influence of summer melt on ice motion after the melt season. Altogether, a high sensitivity of the ratio of summer and fall velocity to summer balance (19% per m w.e. a^{-1}) is found, which implies an increased amplitude of the seasonal velocity cycle, as well as the potential for upward extension of the zone with a pronounced amplitude of the seasonal velocity cycle, in a warming climate. Despite changes in the seasonal velocity signal, annual velocities are found to be insensitive to summer ablation, which suggests a negligible impact of enhanced runoff on mean ice motion.

Acknowledgments
We thank all colleagues that have participated in field campaigns to Nordenskiöldbreen over the years. Financial support for the field activities is provided by the Netherlands Organisation for Scientific Research (NWO), the Swedish Science Council (VR), Stiftelsen Ymer-80, and the Swedish Polar Research Secretariat. Observations during the first years of the project were carried out within the International Polar Year (IPY) framework GLACIODYN. We further acknowledge logistical support provided by the Norwegian Polar Institute. The runoff, velocity, mass balance, and ice thickness data used in this study are available in a data repository (https://doi.org/10.6084/m9.figshare.6176285).

References

Allaart, L. (2016). Combining terrestrial and marine glacial archives: A geomorphological map of the Nordenskioldbreen forefield Svalbard (Master's thesis). Norwegian University of Science and Technology (NTNU).

Andersen, M. L., Larsen, T. B., Nettles, M., Elosegui, P., van As, D., Hamilton, G. S., et al. (2010). Spatial and temporal melt variability at Helheim Glacier, East Greenland, and its effect on ice dynamics. *Journal of Geophysical Research*, *115*, F04041. https://doi.org/10.1029/2010JF001760

Andrews, L. C., Catania, G. A., Hoffman, M. J., Gulley, J. D., Lüthi, M. P., Ryser, C., et al. (2014). Direct observations of evolving subglacial drainage beneath the Greenland Ice Sheet. *Nature*, *514*(7520), 80–83. https://doi.org/10.1038/nature13796

Bartholomaus, T. C., Anderson, R. S., & Anderson, S. P. (2008). Response of glacier basal motion to transient water storage. *Nature Geoscience*, *1*(1), 33–37. https://doi.org/10.1038/ngeo.2007.52

Bartholomew, I., Nienow, P., Mair, D., Hubbard, A., King, M. A., & Sole, A. (2010). Seasonal evolution of subglacial drainage and acceleration in a Greenland outlet glacier. *Nature Geoscience*, *3*(6), 408–411. https://doi.org/10.1038/ngeo863

Bartholomew, I., Nienow, P., Sole, A., Mair, D., Cowton, T., & King, M. A. (2012). Short-term variability in Greenland Ice Sheet motion forced by time-varying meltwater drainage: Implications for the relationship between subglacial drainage system behavior and ice velocity. *Journal of Geophysical Research*, *117*, F03002. https://doi.org/10.1029/2011JF002220

Bingham, R. G., Nienow, P. W., & Sharp, M. J. (2003). Intra-annual and intra-seasonal flow dynamics of a High Arctic polythermal valley glacier. *Annals of Glaciology*, *37*, 181–188. https://doi.org/10.3189/172756403781815762

Bingham, R. G., Nienow, P. W., Sharp, M. J., & Boon, S. (2005). Subglacial drainage processes at a High Arctic polythermal valley glacier. *Journal of Glaciology*, *51*(172), 15–24. https://doi.org/10.3189/172756505781829520

Bintanja, R., Graversen, R. G., & Hazeleger, W. (2011). Arctic winter warming amplified by the thermal inversion and consequent low infrared cooling to space. *Nature Geoscience*, *4*(11), 758–761. https://doi.org/10.1038/ngeo1285

Blatter, H., & Hutter, K. (1991). Polythermal conditions in arctic glaciers. *Journal of Glaciology*, *37*(126), 261–269. https://doi.org/10.3189/S0022143000007279

Bueler, E., & van Pelt, W. (2015). Mass-conserving subglacial hydrology in the Parallel Ice Sheet Model version 0.6. *Geoscientific Model Development*, *8*(6), 1613–1635. https://doi.org/10.5194/gmd-8-1613-2015

Burgess, E. W., Larsen, C. F., & Forster, R. R. (2013). Summer melt regulates winter glacier flow speeds throughout Alaska. *Geophysical Research Letters*, *40*, 6160–6164. https://doi.org/10.1002/2013GL058228

Church, J. A., Monselesan, D., Gregory, J. M., & Marzeion, B. (2013). Evaluating the ability of process based models to project sea-level change. *Environmental Research Letters*, *8*(1), 014051. https://doi.org/10.1088/1748-9326/8/1/014051

Clarke, G. K. (2005). Subglacial processes. *Annual Review of Earth and Planetary Sciences*, *33*(1), 247–276. https://doi.org/10.1146/annurev.earth.33.092203.122621

Cowton, T., Nienow, P., Sole, A., Bartholomew, I., & Mair, D. (2016). Variability in ice motion at a land-terminating Greenlandic outlet glacier: The role of channelized and distributed drainage systems. *Journal of Glaciology*, *62*(233), 451–466. https://doi.org/10.1017/jog.2016.36

Dee, D. P., Uppala, S. M., Simmons, A. J., Berrisford, P., Poli, P., Kobayashi, S., et al. (2011). The ERA-Interim reanalysis: Configuration and performance of the data assimilation system. *Quarterly Journal of the Royal Meteorological Society*, *137*(656), 553–597. https://doi.org/10.1002/qj.828

Den Ouden, M. A. G., Reijmer, C. H., Pohjola, V., Van De Wal, R. S. W., Oerlemans, J., & Boot, W. (2010). Stand-alone single-frequency GPS ice velocity observations on Nordenskiöldbreen, Svalbard. *Cryosphere*, *4*(4), 593–604. https://doi.org/10.5194/tc-4-593-2010

Dunse, T., Schellenberger, T., Hagen, J. O., Kääb, A., Schuler, T. V., & Reijmer, C. H. (2015). Glacier-surge mechanisms promoted by a hydro-thermodynamic feedback to summer melt. *The Cryosphere*, *9*(1), 197–215. https://doi.org/10.5194/tc-9-197-2015

Evans, D. J., & Rea, B. R. (1999). Geomorphology and sedimentology of surging glaciers: A land-systems approach. *Annals of Glaciology*, *28*, 75–82. https://doi.org/10.3189/172756499781821823

Ewertowski, M. W., Evans, D. J. A., Roberts, D. H., & Tomczyk, A. M. (2016). Glacial geomorphology of the terrestrial margins of the tidewater glacier, Nordenskiöldbreen, Svalbard. *Journal of Maps*, *12*(sup1), 476–487. https://doi.org/10.1080/17445647.2016.1192329

Flowers, G. E. (2008). Subglacial modulation of the hydrograph from glacierized basins. *Hydrological Processes*, *22*(19), 3903–3918. https://doi.org/10.1002/hyp.7095

Hewitt, I. (2013). Seasonal changes in ice sheet motion due to melt water lubrication. *Earth and Planetary Science Letters*, *371–372*, 16–25. https://doi.org/10.1016/j.epsl.2013.04.022

Hock, R., & Hooke, R. L. (1993). Evolution of the internal drainage system in the lower part of the ablation area of Storglaciären, Sweden. *Geological Society of America Bulletin*, *105*(4), 537–546. https://doi.org/10.1130/0016-7606(1993)105<0537:EOTIDS>2.3.CO;2

Hoffman, M. J., Andrews, L. C., Price, S. A., Catania, G. A., Neumann, T. A., Lüthi, M. P., et al. (2016). Greenland subglacial drainage evolution regulated by weakly connected regions of the bed. *Nature Communications*, *7*, 13903. https://doi.org/10.1038/ncomms13903

Hubbard, B. P., Sharp, M. J., Willis, I. C., Nielsen, M. K., & Smart, C. C. (1995). Borehole water-level variations and the structure of the subglacial hydrological system of Haut Glacier d'Arolla, Valais, Switzerland. *Journal of Glaciology*, *41*(139), 572–583. https://doi.org/10.3189/S0022143000034894

Iken, A. (1981). The effect of the subglacial water pressure on the sliding velocity of a glacier in an idealized numerical model. *Journal of Glaciology*, *27*(97), 407–421. https://doi.org/10.3198/1981JoG27-97-407-421

Irvine-Fynn, T. D. L., Hodson, A. J., Moorman, B. J., Vatne, G., & Hubbard, A. L. (2011). Polythermal glacier hydrology: A review. *Reviews of Geophysics*, *49*, RG4002. https://doi.org/10.1029/2010RG000350

James, T. D., Murray, T., Barrand, N. E., Sykes, H. J., Fox, A. J., & King, M. A. (2012). Observations of enhanced thinning in the upper reaches of Svalbard glaciers. *The Cryosphere*, *6*(6), 1369–1381. https://doi.org/10.5194/tc-6-1369-2012

Kamb, B. (1987). Glacier surge mechanism based on linked cavity configuration of the basal water conduit system. *Journal of Geophysical Research*, *92*, B99083. https://doi.org/10.1029/JB092iB09p09083

Kamb, B., Engelhardt, H., Fahnestock, M. A., Humphrey, N., Meier, M., & Stone, D. (1994). Mechanical and hydrologic basis for the rapid motion of a large tidewater glacier: 2. Interpretation. *Journal of Geophysical Research*, *99*(B8), 15,231–15,244. https://doi.org/10.1029/94JB00467

Kehrl, L. M., Horgan, H. J., Anderson, B. M., Dadic, R., & Mackintosh, A. N. (2015). Glacier velocity and water input variability in a maritime environment: Franz Josef Glacier, New Zealand. *Journal of Glaciology*, *61*(228), 663–674. https://doi.org/10.3189/2015JoG14J228

Lliboutry, L. (1968). General theory of subglacial cavitation and sliding of temperate glaciers. *Journal of Glaciology*, *7*(49), 21–58. https://doi.org/10.3189/S0022143000020396

Marchenko, S., Pohjola, V. A., Pettersson, R., Van Pelt, W. J. J., Vega, C. P., & Machguth, H. (2016). A plot-scale study of firn stratigraphy at Lomonosovfonna, Svalbard, using ice cores, borehole video and GPR surveys in 2012-14. *Journal of Glaciology*, *63*, 1–12. https://doi.org/10.1017/jog.2016.118

Marchenko, S., Van Pelt, W. J. J., Claremar, B., Pohjola, V., Pettersson, R., Machguth, H., & Reijmer, C. (2017). Parameterizing deep water percolation improves subsurface temperature simulations by a multilayer firn model. *Frontiers in Earth Science*, 5. https://doi.org/10.3389/feart.2017.00016

Nettles, M., Larsen, T. B., Elósegui, P., Hamilton, G. S., & Stearns, L. A. (2008). Step-wise changes in glacier flow speed coincide with calving and glacial earthquakes at Helheim Glacier, Greenland. *Geophysical Research Letters*, *35*, L24503. https://doi.org/10.1029/2008GL036127

Nienow, P., Sharp, M., & Willis, I. C. (1998). Seasonal changes in the morphology of the subglacial drainage system, Haut Glacier d'Arolla, Switzerland. *Earth Surface Processes and Landforms*, *110*(F4), 825–843. https://doi.org/10.1002/(SICI)1096-9837(199809)23:9<825::AID-ESP893>3.0.CO;2-2

Noël, B., van de Berg, W. J., van Meijgaard, E., Kuipers Munneke, P., van de Wal, R. S. W., & van den Broeke, M. R. (2015). Evaluation of the updated regional climate model RACMO2.3: Summer snowfall impact on the Greenland Ice Sheet. *The Cryosphere*, *9*(5), 1831–1844. https://doi.org/10.5194/tc-9-1831-2015

Nuth, C., Kohler, J., König, M., Von Deschwanden, A., Hagen, J. O., Kääb, A., et al. (2013). Decadal changes from a multi-temporal glacier inventory of Svalbard. *The Cryosphere*, *7*(5), 1603–1621. https://doi.org/10.5194/tc-7-1603-2013

Nuttall, A.-M., & Hodgkins, R. (2005). Temporal variations in flow velocity at Finsterwalderbreen, a Svalbard surge-type glacier. *Annals of Glaciology*, *42*(1), 71–76. https://doi.org/10.3189/172756405781813140

Oerlemans, J., & Van Pelt, W. J. J. (2015). A model study of Abrahamsenbreen, a surging glacier in northern Spitsbergen. *The Cryosphere*, *9*(2), 767–779. https://doi.org/10.5194/tc-9-767-2015

Parizek, B. R., & Alley, R. B. (2004). Implications of increased Greenland surface melt under global-warming scenarios: Ice-sheet simulations. *Quaternary Science Reviews*, *23*(9-10), 1013–1027. https://doi.org/10.1016/j.quascirev.2003.12.024

Rachlewicz, G., Szczucinski, W., & Ewertowski, M. (2007). Post-Little Ice Age retreat rates of glaciers around Billefjorden in central Spitsbergen, Svalbard. *Polish Polar Research*, *28*(3), 159–186.

Röthlisberger, H. (1972). Water pressure in intra- and subglacial channels. *Journal of Glaciology*, *11*(62), 177–203. https://doi.org/10.1017/S0022143000022188

Schoof, C. (2010). Ice-sheet acceleration driven by melt supply variability. *Nature*, *468*(7325), 803–806. https://doi.org/10.1038/nature09618

Serreze, M. C., Barrett, A. P., Stroeve, J. C., Kindig, D. N., & Holland, M. M. (2009). The emergence of surface-based Arctic amplification. *The Cryosphere*, *3*(1), 11–19. https://doi.org/10.5194/tc-3-11-2009

Sevestre, H., & Benn, D. I. (2015). Climatic and geometric controls on the global distribution of surge-type glaciers: Implications for a unifying model of surging. *Journal of Glaciology*, *61*(228), 646–662. https://doi.org/10.3189/2015JoG14J136

Sole, A., Nienow, P., Bartholomew, I., Mair, D., Cowton, T., Tedstone, A., & King, M. A. (2013). Winter motion mediates dynamic response of the Greenland Ice Sheet to warmer summers. *Geophysical Research Letters*, *40*, 3940–3944. https://doi.org/10.1002/grl.50764

Stevens, L. A., Behn, M. D., Das, S. B., Joughin, I., Noël, B. P. Y., van den Broeke, M. R., & Herring, T. (2016). Greenland Ice Sheet flow response to runoff variability. *Geophysical Research Letters*, *43*, 11,295–11,303. https://doi.org/10.1002/2016GL070414

Sundal, A. V., Shepherd, A., Nienow, P., Hanna, E., Palmer, S., & Huybrechts, P. (2011). Melt-induced speed-up of Greenland ice sheet offset by efficient subglacial drainage. *Nature*, *469*(7331), 521–524. https://doi.org/10.1038/nature09740

Tedstone, A. J., Nienow, P. W., Gourmelen, N., Dehecq, A., Goldberg, D., & Hanna, E. (2015). Decadal slowdown of a land-terminating sector of the Greenland Ice Sheet despite warming. *Nature*, *526*(7575), 692–695. https://doi.org/10.1038/nature15722

Thomson, L., & Copland, L. (2017). Multi-decadal reduction in glacier velocities and mechanisms driving deceleration at polythermal White Glacier, Arctic Canada. *Journal of Glaciology*, *63*(239), 450–463. https://doi.org/10.1017/jog.2017.3

Vallot, D., Pettersson, R., Luckman, A., Benn, D. I., Zwinger, T., Van Pelt, W. J. J., et al. (2017). Basal dynamics of Kronebreen, a fast-flowing tidewater glacier in Svalbard: Non-local spatio-temporal response to water input. *Journal of Glaciology*, *63*(242), 1012–1024. https://doi.org/10.1017/jog.2017.69

Van Pelt, W. J. J., & Kohler, J. (2015). Modelling the long-term mass balance and firn evolution of glaciers around Kongsfjorden, Svalbard. *Journal of Glaciology*, *61*(228), 731–744. https://doi.org/10.3189/2015JoG14J223

Van Pelt, W. J. J., Kohler, J., Liston, G. E., Hagen, J. O., Luks, B., Reijmer, C. H., & Pohjola, V. A. (2016). Multidecadal climate and seasonal snow conditions in Svalbard. *Journal of Geophysical Research: Earth Surface*, *121*, 2100–2117. https://doi.org/10.1002/2016JF003999

Van Pelt, W. J. J., Oerlemans, J., Reijmer, C. H., Pettersson, R., Pohjola, V. A., Isaksson, E., & Divine, D. (2013). An iterative inverse method to estimate basal topography and initialize ice flow models. *The Cryosphere*, *7*(3), 987–1006. https://doi.org/10.5194/tc-7-987-2013

Van Pelt, W. J. J., Oerlemans, J., Reijmer, C. H., Pohjola, V. A., Pettersson, R., & Van Angelen, J. H. (2012). Simulating melt, runoff and refreezing on Nordenskiöldbreen, Svalbard, using a coupled snow and energy balance model. *The Cryosphere*, *6*(3), 641–659. https://doi.org/10.5194/tc-6-641-2012

Van Pelt, W. J. J., Pettersson, R., Pohjola, V. A., Marchenko, S., Claremar, B., & Oerlemans, J. (2014). Inverse estimation of snow accumulation along a radar transect on Nordenskiöldbreen, Svalbard. *Journal of Geophysical Research: Earth Surface*, *119*, 816–835. https://doi.org/10.1002/2013JF003040

Van Pelt, W. J. J., Pohjola, V. A., & Reijmer, C. H. (2016). The changing impact of snow conditions and refreezing on the mass balance of an idealized Svalbard glacier. *Frontiers in Earth Science*, *4*(102). https://doi.org/10.3389/feart.2016.00102

Van de Wal, R. S. W., Boot, W., van den Broeke, M. R., Smeets, C., Reijmer, C. H., Donker, J. J. A., & Oerlemans, J. (2008). Large and rapid melt-induced velocity changes in the ablation zone of the Greenland Ice Sheet. *Science*, *321*(5885), 111–113. https://doi.org/10.1126/science.1158540

Van de Wal, R. S. W., Smeets, C. J. P. P., Boot, W., Stoffelen, M., van Kampen, R., Doyle, S. H., & Wilhelms, F. (2015). Self-regulation of ice flow varies across the ablation area in south-west Greenland. *The Cryosphere*, *9*(2), 603–611. https://doi.org/10.5194/tc-9-603-2015

Vega, C. P., Pohjola, V. A., Beaudon, E., Claremar, B., Van Pelt, W. J. J., Pettersson, R., et al. (2016). A synthetic ice core approach to estimate ion relocation in an ice field site experiencing periodical melt: A case study on Lomonosovfonna, Svalbard. *The Cryosphere*, *10*(3), 961–976. https://doi.org/10.5194/tc-10-961-2016

Waechter, A., Copland, L., & Herdes, E. (2015). Modern glacier velocities across the Icefield Ranges, St Elias Mountains, and variability at selected glaciers from 1959 to 2012. *Journal of Glaciology*, *61*(228), 624–634. https://doi.org/10.3189/2015JoG14J147

Walder, J. S. (1986). Hydraulics of subglacial cavities. *Journal of Glaciology*, *32*(112), 439–445. https://doi.org/10.3189/S0022143000012156

Werder, M. A., Hewitt, I. J., Schoof, C. G., & Flowers, G. E. (2013). Modeling channelized and distributed subglacial drainage in two dimensions. *Journal of Geophysical Research: Earth Surface*, *118*, 2140–2158. https://doi.org/10.1002/jgrf.20146

Zwally, H. J., Abdalati, W., Herring, T., Larson, K., Saba, J., & Steffen, K. (2002). Surface melt-induced acceleration of Greenland ice-sheet flow. *Science (New York, N.Y.)*, *297*(5579), 218–222. https://doi.org/10.1126/science.1072708